Molecular dynamics simulation study of deposition and annealing behaviors of Al atoms on Cu surface

S.-P. Kim,[1] K.-R. Lee,[1,a)] Y.-C. Chung,[2] M. Sahashi,[3] and Y. K. Kim[4]
[1]*Computational Science Center, Convergence Technology Laboratory, Korea Institute of Science and Technology, Seoul 136-791, Republic of Korea*
[2]*Division of Materials Science Engineering, Hanyang University, Seoul 133-791, Republic of Korea*
[3]*Department of the Electronic Engineering, Tohoku University, Sendai 980-8579, Japan*
[4]*Department of Materials Science and Engineering, Korea University, Seoul 136-713, Republic of Korea*

(Received 10 March 2009; accepted 3 May 2009; published online 8 June 2009)

Deposition and annealing behaviors of Al atoms on rough Cu (111) surface were investigated on the atomic scale by three-dimensional classical molecular dynamics simulation. The rough Cu surface was modeled by depositing 5 ML of Cu on Ta (011) substrate. Most Al atoms deposited on the rough Cu surface placed on the atomic steps, preserving the major features of the surface during Al deposition. This behavior was discussed in terms of the smaller barrier of the surface diffusion than Ehrlich–Schwoebel barrier of Al on Cu (111) surface. By annealing at 700 K, significant intermixing between Al and Cu rapidly occurs with decrease in the surface roughness. This behavior reveals that the exchange process of Al with substrate Cu dominates during the initial stage of high temperature annealing. © *2009 American Institute of Physics*. [DOI: 10.1063/1.3142382]

I. INTRODUCTION

Current-confined-path current-perpendicular-to-plane giant magnetoresistance (CPP-GMR) device was suggested to have higher magnetic resistance (MR) value than that of conventional CPP-GMR device.[1] The device has a unique microstructure of the thin oxide layer between two ferromagnetic thin films. Metallic conduction paths of diameter, a few nanometers, are scattered in the oxide layer, which plays a role as the confined current path. This device has drawn much attention owing to its potential application to the read head of the next generation data storage system, which can exhibit the low Johnson noise feature at high speed data transfer rate. The first realization of the device using Al_2O_3–Cu nano-oxide layer (NOL) was reported by Fukuzawa *et al.*[2–4] They showed that the MR ratio of the GMR device with the NOL increased, while the resistance of the area contact was kept small presumably due to confining the spin movement in the current confined path. Controlling the size and the distribution of nanometallic channel inside the NOL is thus essential to optimize the device performance.

Al–Cu thin film system is widely used for the channel layer of the GMR device because the chemical affinity to oxygen is greatly different between Al and Cu. Exposed to an oxidation environment, Al will be easily oxidized, whereas Cu will form nanometallic channels of the NOL. Systematic control of the atomic structure of the NOL needs understanding of the surface structure and the deposition kinetics of Al atoms on the Cu surface. Recently, Soh and co-workers[5,6] employed scanning probe microscopy analysis to identify the current-confined-path in the Al_2O_3–Cu NOL using the thin film stack consisted of Ta(5 nm)/Cu(10 nm)/Al(0.2 nm =1 ML). However, quantitative understanding of the atomic structure and composition of the surface is still challenging due to the limits of the experimental analysis.

Molecular dynamics (MD) simulation using valid interatomic potentials provides the quantitative information on deposition, diffusion, thermal, and mechanical properties in atomic scale. MD simulation has been employed in many metallic thin film systems to understand the surface or interface phenomena and to suggest a kinetic model to explain the puzzling experimental observations.[7–11] In the present work, we studied the deposition behavior of Al on Cu surface by classical MD simulation with embedded atom method (EAM) potential for Al and Cu. For more realistic simulation, we prepared a rough Cu surface of (111) orientation by simulating the deposition of 5 ML of Cu on Ta (011) surface. Details of the Al deposition on the rough Cu surface and the surface reaction during thermal annealing at 700 K are reported in atomic scale.

II. COMPUTATIONAL PROCEDURE

In order to model the Cu substrate surface, five layers of Cu were deposited on a Ta (011) surface using MD simulation. Structural compatibility between *bcc* Ta (011) and *fcc* Cu (111) surfaces enhanced the formation of (111) textured Cu substrate. On the Cu/Ta substrate, Al atoms up to 1 ML (8000 atoms) were deposited. Semiempirical EAM potentials of Cu–Al and Cu–Ta systems were used for the simulation.[12,13] The potentials were rigorously benchmarked by using the calculated or experimentally observed physical properties of the elements and their intermetallic compounds as summarized in Table I.

Single crystal bcc Ta of the size approximately $33 \times 18.7 \times 4.5\ nm^3$ was used as the substrate. The substrate is composed of 160 000 Ta atoms with the (011) surface normal to z direction. Periodic boundary condition was applied in both x and y directions. No defects or steps were artificially

a)Electronic mail: krlee@kist.re.kr.

 © 2009 American Institute of Physics

Author complimentary copy. Redistribution subject to AIP license or copyright, see http://jap.aip.org/jap/copyright.jsp

TABLE I. Properties of Al, Cu, Ta, and their intermetallic compounds predicted by EAM potentials employed in this study in comparison with experimental data from literatures.

	Al		Al_3Cu		$AlCu_3$		Cu		Ta	
Property	Expt. or DFT	Calc.	Expt. or DFT	Calc.	Expt. or DFT	Calc.	Expt. or DFT	Calc.	Expt. or DFT	Calc.
Structure	fcc (A1)		$L1_2$		$L1_2$		fcc (A1)		bcc (A2)	
a_0 (Å)	4.05[a]	4.05	3.94[b]	3.95	3.72[b]	3.74	3.615[a]	3.614	3.301[a]	3.303
E_{coh} (eV)	3.36[a]	3.58	⋯	3.66	⋯	3.64	3.52[a]	3.54	8.10[a]	8.092
B (GPa)	76[c]	78.76	⋯	95.78	⋯	86.62	140[c]	133.18	200[c]	189.7
C' (GPa)	26[c]	16.24	⋯	21.23	⋯	4.81	48[c]	24.44	69[c]	51.11
γ_{111} (mJ/m^2)	935[d]	779.64	⋯	966.46	⋯	1321.44	1952[d]	1502.64	3455[d]	2758.78
γ_{100} (mJ/m^2)	1081[d]	831.97	⋯	1034.73	⋯	1383.41	2166[d]	1563.62	3097[d]	2411.7
γ_{110} (mJ/m^2)	1090[d]	953.82	⋯	1153.10	⋯	1536.66	2237[d]	1754.24	3084[d]	2008.7

[a]Reference 22.
[b]The values are from the prediction of Vegard's law.
[c]Reference 23.
[d]Reference 24.

introduced into the substrate surface. The atomic positions of the bottom three layers were fixed to simulate a thick substrate. Temperature of the next nine layers was rescaled at 300 K in every 100 MD steps, so that the layers could act as a thermal bath during deposition. All the other atoms were unconstrained with initial temperature of 300 K. The substrate was equilibrated by MD relaxation until the temperature of the substrate fluctuated within 300 ± 10 K. Cu atoms were then deposited in a direction normal to the surface or $-z$ direction. Initial position of the deposited atom was randomly selected in the x-y plane distanced by 4.67 nm from the substrate surface. The kinetic energy of the deposited atoms was set to 0.1 eV, which is typical of that found in evaporation or molecular beam epitaxial growth. We used relatively low initial kinetic energy of the deposited atom to prevent damages on the substrate surface, which enabled us to investigate the details of the interaction between the adatom and the surface structure. Simulation condition for the Al deposition was the same as that of the Cu deposition on the Ta surface. The time step for the MD simulation was 1.0 fs. The time interval between two consecutive depositions was fixed at 1 ps. Prior to simulating next deposition event, the temperature of the substrates was rescaled to 300 K after the rearrangement of the deposited atom had settled down. This compulsive rescaling and deposition method results in an accelerated simulation of the deposition process. Therefore, the deposition rate and the simulation time of the simulation cannot correspond to the real values. Although this acceleration procedure may have an effect to neglect the atomic reaction in long time scale, it is hardly observed that further reaction after the settlement occurs at room temperature. All simulations were performed by using the large-scale atomic/molecular massively parallel simulator code.[14]

III. RESULTS AND DISCUSSION

Figure 1 shows the Cu film evolution as 5 ML of Cu were deposited on a Ta (011) surface. The first deposited layer of Cu exhibits the typical of layer-by-layer growth mode. When 0.5 ML of Cu was deposited, small Cu islands were formed on the surface. The Cu islands laterally grew until the Ta (011) surface was covered by the monolayer of deposited Cu atoms. Because of the size difference between Cu and Ta (first nearest neighbor distance: 2.56 Å for Cu, 2.86 Å for Ta), the Ta surface was completely covered when 1.07 ML of Cu were deposited. No interfacial intermixing in atomic scale was observed, which is in good agreement with previous simulation results.[15,16] Further deposition of Cu resulted in a contrasting surface morphology to the first layer of Cu on Ta (011) surface. Comparing the microstructures between 2 and 0.5 ML of Cu deposition cases, it is evident that the size of Cu islands on Cu was much larger than those on Ta (011) substrate. In addition, three-dimensional islands started to form on the large Cu islands as indicated by arrows. As the deposition of Cu proceeded, three-dimensional islands of Cu evolved to form a rough Cu surface. Analysis of the surface roughness shown in Fig. 2 also shows the change in the growth mode. At the initial stage of the Cu deposition (<1 ML), the roughness varies in the typical layer-by-layer growth mode. As the deposited Cu layer increases, the surface roughness monotonically increases with the three-dimensional island formation.

This structure evolution can be elucidated in terms of the energy barriers for surface diffusion and Ehrlich–Schwoebel (ES) barriers. The energy barrier was obtained by using molecular static calculation along the most feasible diffusion path on the surface. Energy barrier of Cu surface diffusion in $[3\bar{2}2]$ direction on Ta (011) surface is 0.29 eV. However, the barrier in $[11\bar{2}]$ direction on Cu (111) surface is much smaller (0.11 eV). Even on the strained Cu (111) surface, caused by the lattice mismatch between Cu and Ta, the barrier is only 0.15 eV. Therefore, the Cu atoms on the Cu (111) surface would diffuse faster than those on the Ta (011) surface, which resulted in the formation of larger islands on Cu (111) surface (see 2 ML Cu deposition case in Fig. 1). On the other hand, ES barrier for a Cu atom to move across the Cu step on the Cu (111) surface is 0.53 eV. This value is larger than that for the Cu step on the Ta (011) surface (0.44 eV). It is thus expected that on the Cu (111) surface, the deposited Cu atoms that arrived on the terrace of the previously formed Cu islands would rapidly diffuse to form other islands on that terrace rather than moving across the Cu step to the lower Cu surface. On the Ta (011) surface, Cu atoms that arrived on

Author complimentary copy. Redistribution subject to AIP license or copyright, see http://jap.aip.org/jap/copyright.jsp

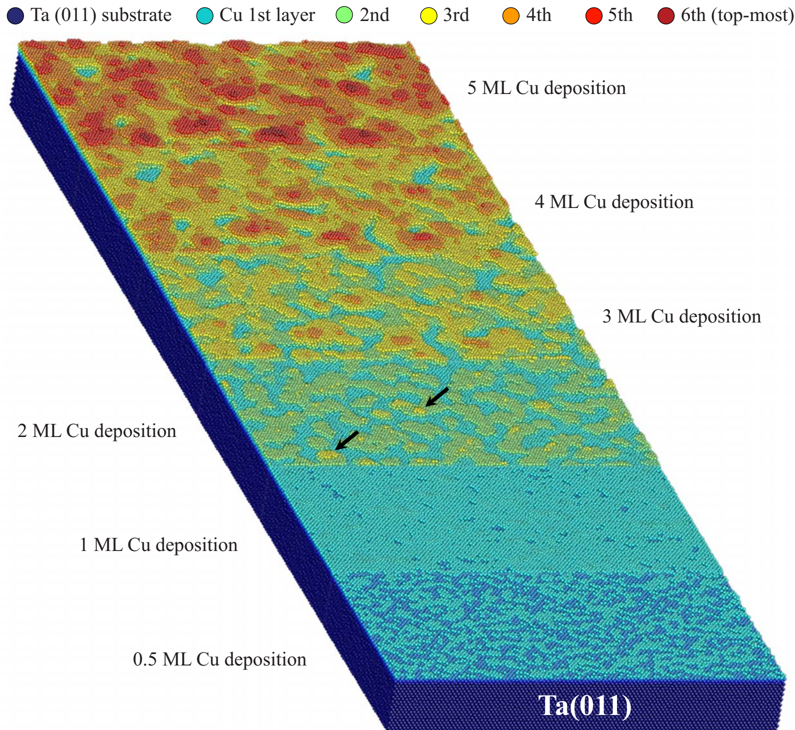

FIG. 1. (Color online) Atomic scale surface structure evolution during Cu deposition on Ta (011) surface at room temperature.

the terrace of Cu island can cross the step with less difficulty due to the lower ES barrier and the smaller size of the Cu island.

Deposition behavior of the Al adatoms on the rough Cu surface was illustrated in Fig. 3 for the cases of 0.25 ML (a) and 0.5 ML (b) depositions. Al atoms are presented by gray circle, while Cu atoms are presented by various colors according to the layer number counting from the Ta (011) surface. It is evident from Fig. 3(a) that most of deposited Al atoms are placed on the step of each Cu layer. As the deposition proceeded, the Al layer started to cover the Cu terrace growing from the steps [see the area marked by A in Figs. 3(a) and 3(b)]. Similar deposition behavior was observed in the trench region marked by B in Fig. 3. Deposited Al atoms diffuse to the surrounding Cu steps before growing on the bottom surface of the trench. However, it is noted that the number of Al atoms on the bottom of the trench is relatively small, which can increase the surface roughness as will be discussed later. This behavior is presumably due to the steering effect[17] that the deposited atoms are attracted toward the adjacent steps or islands near the surface, which impedes the Al atoms from the deposition on the bottom of the trench.

Kim *et al.*[18] studied the Al deposition behavior on various orientations of Cu surface with artificial Cu plateau at room temperature. Even in short duration of 1 ps after deposition, the Al atoms on Cu (111) surface diffuse rapidly to be placed on a stable site such as Cu or Al steps. The Al atoms deposited on the plateau tend to form a large Al cluster on

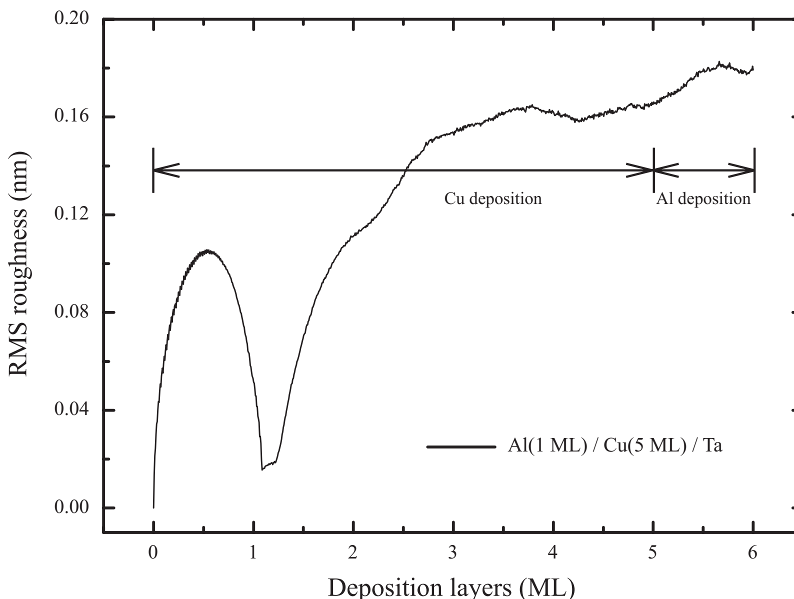

FIG. 2. Change in rms value of surface roughness during Cu deposition on Ta (011) surface and consecutive Al deposition on the Cu surface.

Author complimentary copy. Redistribution subject to AIP license or copyright, see http://jap.aip.org/jap/copyright.jsp

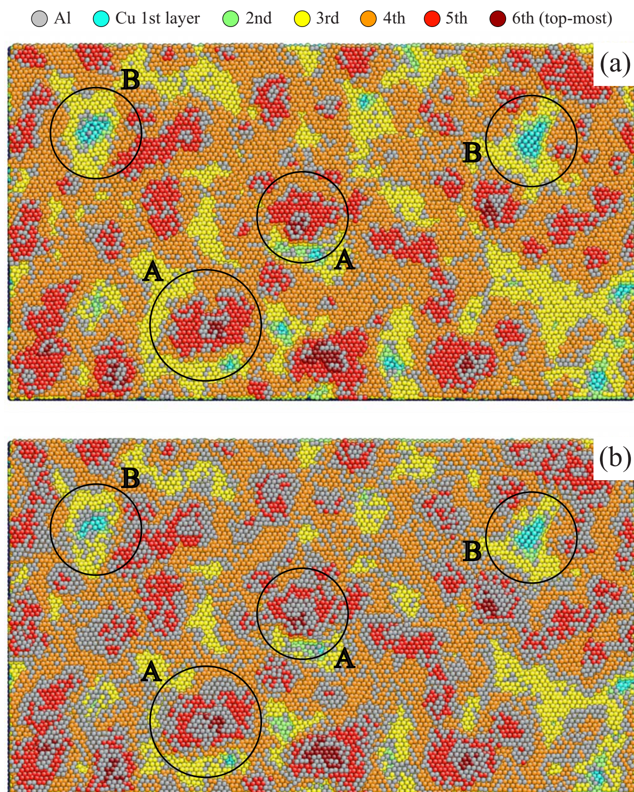

FIG. 3. (Color online) Atomic scale surface structure after 0.25 ML of Al (a) and 0.5 ML of Al (b) depositions on the rough Cu (111) surface.

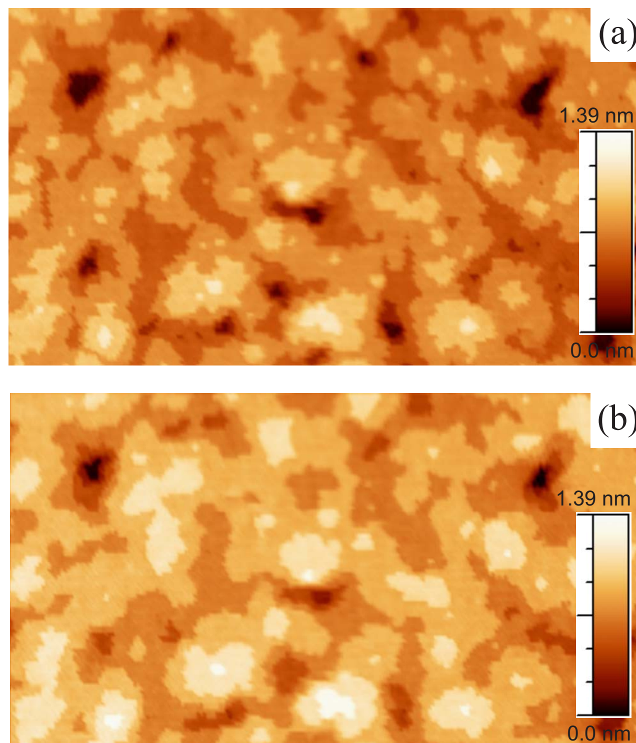

FIG. 4. (Color online) Isopotential contour of the surface before (a) and after (b) 1 ML of Al deposition on the rough Cu (111) surface.

the plateau rather than cross over the ES barrier. They showed that this behavior originates from the higher value of ES barrier, 0.28 eV than that of the surface diffusion barrier, 0.055 eV. Deposition behavior observed in the present work is in good agreement with those of the previous simulations.[18]

Figure 4 shows the isopotential contour of the surface or simulated atomic force microscope image before and after depositing 1 ML of Al on the Cu surface. The height of the surface with respect to the lowest point of the surface is presented by the brightness. The isopotential contour was obtained by calculating a set of points above the surface at which the force in the z-direction on a virtual single atom probe is zero.[19] Topography of the surface was basically preserved: all trenches and hills persist after the Al deposition. However, rms value of the surface roughness (see Fig. 2) reveals that the Al deposition slightly increased the roughness. The increase in the surface roughness during Al deposition seems to originate from the steering effect discussed in Fig. 3.

In order to examine the atomic scale surface reaction during thermal annealing, the Al deposited Cu thin film was annealed at various temperatures from 400 to 1000 K. Only the annealing behavior at 700 K will be reported in the present paper because observable changes in the surface structure occurred in the present MD time scale when the annealing temperature was higher than 700 K. Annealing behavior at 1000 K was essentially the same as those at 700 K except the faster kinetic rate. Figure 5 shows the change in surface topography (left) and atomic configuration (right) with the annealing time. In the atomic configurations, yellow circle presents Cu atom and gray circle Al atom. As can be seen in the left column of Fig. 5, the surface roughness noticeably decreased with the annealing: rms surface roughness decreased from 0.18 to 0.14 nm after 2.0 ns of the annealing at 700 K. It is also obvious that the reduction in the surface roughness was accompanied by the homogenization of the surface composition. On the surface of as deposited specimen, Al atoms were segregated on the hill [for example, see region B of Fig. 5(a)] than the trench (for example, see region A). However, the segregation distinctly fades away in a few nanoseconds by thermal annealing at 700 K as shown in Figs. 5(b) and 5(c). Fractions of pair type between the nearest-neighbor atoms were calculated to quantify the degree of the intermixing during annealing. Table II summarizes the fractions of Al–Al, Cu–Cu, and Al–Cu pairs of the films before and after annealing simulation. Because the thickness of Cu layer (5 ML) is much larger than that of Al, the fraction of Cu–Cu pair is the largest in as deposited film. After the annealing, the fractions of Al–Al and Cu–Cu pair decreased from 7.2% to 6.8% and 79.1% to 77.4%, respectively. However, the fraction of Al–Cu pair increased from 13.7% to 15.8%, which supports the intermixing during annealing.

It is evident in Fig. 5 that the reduction in the surface roughness and the intermixing between Al and Cu surface atoms occur simultaneously during the initial stage of annealing at 700 K. This simultaneous reaction can occur by the exchange process of Al with substrate Cu atom, where the deposited Al atom penetrates into the Cu plateau with protrusion of a Cu atom in the periphery of the Cu step. Mo *et al.*[20] investigated the energetics of adatom interaction with

Author complimentary copy. Redistribution subject to AIP license or copyright, see http://jap.aip.org/jap/copyright.jsp

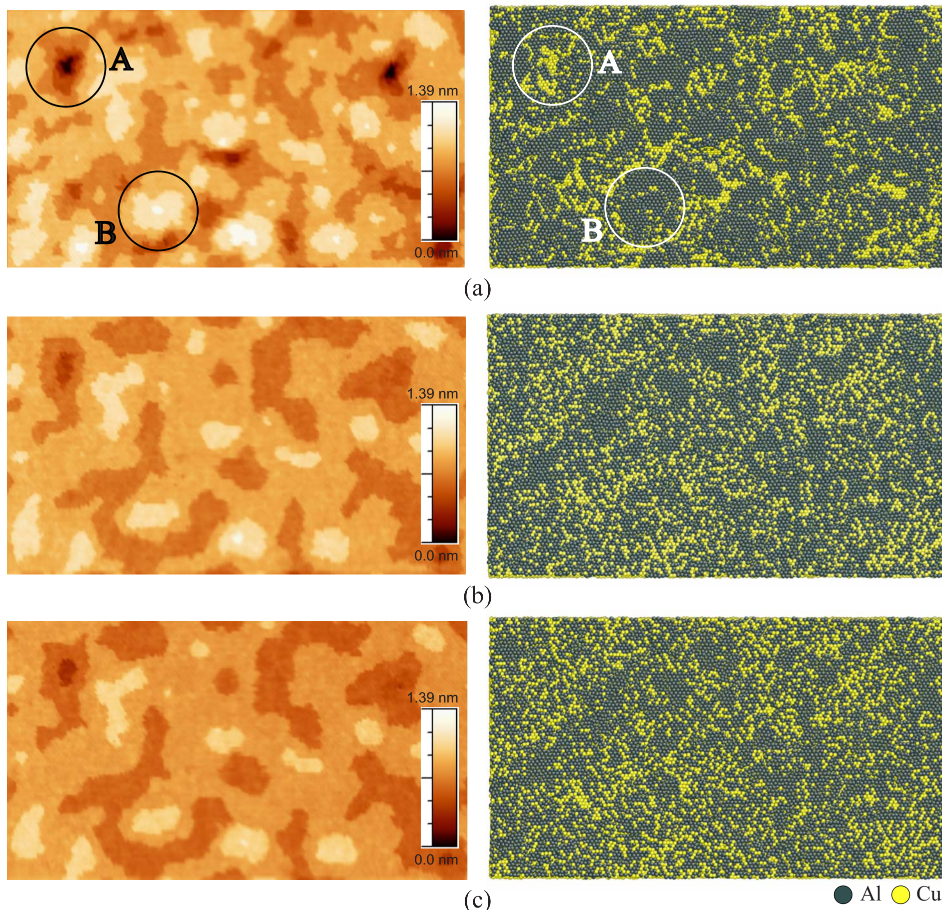

FIG. 5. (Color online) Changes in isopotential contour of the surface and compositional surface configuration during annealing at 700 K, (a) as deposited surface, (b) after 1 ns of annealing, and (c) after 2 ns of annealing.

the step on Cu (111) and Pd (111) surface by employing first-principles calculations with nudged elastic band method. They found that the energy barrier for the exchange process is smaller than that of hopping process when the bonding between adatom and substrate atom is strong. Cu–Al system has various stable intermetallic compound phases,[21] which results from a large binding energy between Cu and Al. By the MD simulation of annealing in the simplified Al–Cu system, Kim *et al.*[18] actually showed that the exchange process of Al has much smaller energy barrier (0.106 eV) than hopping process across the ES barrier (0.331 eV) on Cu (111) surface. It must be further noted that the exchange process can readily occur on the closely packed Cu (111) surface because of the smaller barrier of the surface diffusion of Cu on the Cu (111) surface.

The present simulation result would suggest a kinetic model to generate the Cu nanoconducting path in Al_2O_3 NOL layer. Thermal annealing after Cu–Al deposition or alloy deposition of Cu–Al is commonly used in the process for preparing current-confined-path CCP-CPP spin valve devices.[2–6] Hence, the compositionally uniform Cu–Al surface layer is expected to form either by the exchange process during annealing or chemical alloying between Cu and Al. Subsequent oxidation of the compositionally uniform Al–Cu surface layer will cause phase separation between aluminum oxide and pure Cu phase because the solubility of Cu in aluminum oxide phase is negligible. Microstructure of the NOL would be governed by the phase separation behavior during oxidation of Al–Cu alloy. Atomic scale simulation of oxidation behavior of the Al–Cu alloy surface would be thus invaluable, even if it is challenging to study the large scale phase separation behavior by atomic scale simulation.

TABLE II. The fractions of pair type between the nearest-neighbor atoms.

Pair	As dep.	After annealing 2 ns at 700 K
Al–Al	7.2%	6.8%
Al–Cu	13.7%	15.8%
Cu–Cu	79.1%	77.4%

IV. CONCLUSION

Thin film growth and annealing behaviors of Al–Cu thin film system was investigated in atomic scale by using massive MD simulation. A rough Cu surface modeled by MD simulation of 5 ML Cu deposition on Ta (011) surface enabled us to study the Al deposition behavior on more realistic Cu (111) surface. On the rough Cu (111) surface, most Al adatoms are placed on the step or on the plateaus of Cu surface preserving the Cu surface topography. However, thermal annealing of the sample at 700 K significantly reduces the surface roughness simultaneously with the intermixing of Al and Cu surface atoms. This annealing behavior would result from significant exchange process of Al with substrate Cu atoms, as can be expected by comparing the energy barriers between the exchange process and the hopping process across the Cu step. It was suggested that the Cu

Author complimentary copy. Redistribution subject to AIP license or copyright, see http://jap.aip.org/jap/copyright.jsp

nanochannels in NOL can be generated by the phase separation of aluminum oxide and pure Cu during oxidation of the uniform Al–Cu surface layer.

ACKNOWLEDGMENTS

This work was financially supported by the KIST research program for the enhancement of research capability, Project No. 2E21040. This work was also supported by the Korea Science and Engineering Foundation, Grant No. M10500000105-05J0000-10510 and the Korea Foundation for International Cooperation of Science & Technology, Grant No. M60501000045-05A0100-04510.

[1]M. Takagishi, K. Koi, M. Yoshikawa, T. Funayama, H. Iwasaki, and M. Sahashi, IEEE Trans. Magn. **38**, 2277 (2002).
[2]H. Fukuzawa, H. Yuasa, S. Hashimoto, K. Koi, H. Iwasaki, M. Takagishi, Y. Tanaka, and M. Sahashi, IEEE Trans. Magn. **40**, 2236 (2004).
[3]H. Fukuzawa, H. Yuasa, S. Hashimoto, H. Iwakaki, and Y. Tanaka, Appl. Phys. Lett. **87**, 082507 (2005).
[4]H. Fukuzawa, H. Yuasa, K. Koi, H. Iwasaki, Y. Tanaka, Y. K. Takahashi, and K. Hono, J. Appl. Phys. **97**, 10C509 (2005).
[5]J. Y. Soh, S.-P. Kim, Y. K. Kim, K.-R. Lee, Y.-C. Chung, S. Kawasaki, K. Miyake, M. Doi, and M. Sahashi, IEEE Trans. Magn. **42**, 2633 (2006).
[6]S. Kawasaki, J. Soh, K. Miyake, M. Doi, and M. Sahashi, J. Magn. Soc. Jpn. **30**, 357 (2006).
[7]W. Zhu, F. B. de Mongeot, U. Valbusa, E. G. Wang, and Z. Zhang, Phys. Rev. Lett. **92**, 106102 (2004).
[8]S. Durukanoğlu, O. S. Trushin, and T. S. Rahman, Phys. Rev. B **73**, 125426 (2006).
[9]G. Bozzolo, J. E. Garcés, and G. Demarco, Surf. Sci. **532–535**, 41 (2003).
[10]R. Pentcheva, K. A. Fichthorn, M. Scheffler, T. Bernhard, R. Pfandzelter, and H. Winter, Phys. Rev. Lett. **90**, 076101 (2003).
[11]S.-P. Kim, S.-C. Lee, K.-R. Lee, and Y.-C. Chung, Acta Mater. **56**, 1011 (2008).
[12]M. S. Daw and M. I. Baskes, Phys. Rev. B **29**, 6443 (1984).
[13]X. W. Zhou, R. A. Jonson, and H. N. G. Wadley, Phys. Rev. B **69**, 144113 (2004).
[14]LAMMPS, Sandia National Laboratories, 2008, http://lammps.sandia.gov/.
[15]T. P. C. Klaver and B. J. Thijsse, J. Comput.-Aided Mater. Des. **10**, 61 (2003).
[16]M. F. Francis, M. N. Neurock, X. W. Zhou, J. J. Quan, H. N. G. Wadley, and E. B. Webb III, J. Appl. Phys. **104**, 034310 (2008).
[17]F. Montalenti and A. F. Voter, Phys. Rev. B **64**, 081401 (2001).
[18]S.-P. Kim, K.-R. Lee, Y.-C. Chung, Y. K. Kim, M. Doi, and M. Sahashi, J. Korean Phys. Soc. **52**, 1241 (2008).
[19]N. Kalyanasundaram, J. B. Freund, and H. T. Johnson, ASME J. Eng. Mater. Technol. **127**, 457 (2005).
[20]Y. Mo, W. Zhu, E. Kaxiras, and Z. Zhang, Phys. Rev. Lett. **101**, 216101 (2008).
[21]*ASM Handbook: Alloy Phase Diagrams* (ASM International, Materials Park, OH, 1990), Vol. 3.
[22]W. F. Gale and T. C. Totemeier, *Smithells Metal Reference Book*, 8th ed. (Elsevier Butterworth-Heinemann, Oxford, 2004).
[23]G. Simmons and H. Wang, *Single Crystal Elastic Constants and Calculated Aggregate Properties: A Handbook* (MIT, Cambridge, 1971).
[24]L. Vitos, A. V. Ruban, H. L. Skriver, and J. Kollar, Surf. Sci. **411**, 186 (1998).

Author complimentary copy. Redistribution subject to AIP license or copyright, see http://jap.aip.org/jap/copyright.jsp